LAWRENCE
LIVERMORE
NATIONAL
LABORATORY

UCRL-JRNL-200058

Local Structure of amorphous (PbO)x[(B2O3)1-z(Al2O3)z]y (SiO2)y Dielectric Materials by Multinuclear Solid State NMR

A. Sawvel, S. Chinn, W. Bourcier, R. Maxwell

September 9, 2003

Chemistry of Materials

UCRL-JRNL-200058

Local Structure of Amorphous $(PbO)_x [(B_2O_3)_{1-z} (Al_2O_3)_z]_y (SiO_2)_y$ Dielectric Materials by Multinuclear Solid State NMR

April M. Sawvel[†], Sarah C. Chinn[‡], William L. Bourcier[†], Robert S. Maxwell[‡,]*

[†]Energy and Environment, Lawrence Livermore National Laboratory, 7000 East Avenue, L-221, Livermore, CA 94551, USA

[‡]Chemistry and Materials Science, Lawrence Livermore National Laboratory, 7000 East Avenue, L-231, Livermore, CA 94551, USA

Abstract

Structural speciation of glasses in the systems PbO-B_2O_3-SiO_2, PbO-B_2O_3-Al_2O_3-SiO_2, and PbO-Al_2O_3-SiO_2 were studied using solid-state ^{29}Si, ^{27}Al, ^{11}B, and ^{207}Pb nuclear magnetic resonance (NMR) and Raman spectroscopy. Application of these methods provided insight into the role of Al_2O_3 incorporation in the lead-borosilicate glass networks. The general composition range studied was $(PbO)_x [(B_2O_3)_{1-z} (Al_2O_3)_z]_y (SiO_2)_y$ where x = 0.35, 0.5, and 0.65, y = (1-x)/2 and z = 0.0, 0.5 and 1.0. Additional insight was obtained via ^{27}Al 2D-3QMAS experiments. The ^{207}Pb spin echo mapping spectra showed a transition from ionic (Pb^{2+}) to covalently bound lead species with increased PbO contents in the borosilicate glasses. The addition of aluminum to the glass network further enhanced the lead species transition resulting in a higher relative amount of covalent lead bonding in the high PbO content alumino-borosilicate glass. The

* To whom correspondence should be addressed. E-mail: maxwell7@llnl.gov. Tel: (925) 423-4991. Fax: (925) 423-8772.

number of BO_4 units present in the ^{11}B MAS NMR decreased with increasing PbO contents for both the borosilicate and the alumino-borosilicate glass systems, with the addition of aluminum further promoting the BO_3 species. A deshielding of the ^{11}B chemical shifts and the ^{27}Al chemical shifts with increased lead contents (independent of changes in the quadrupolar coupling) was also observed for both glass systems and was attributed to increasingly homogeneous glass structure. The ^{29}Si spectra of the borosilicate and alumino-borosilicate glasses showed a downfield shift with increased PbO concentrations representing incorporation of Pb into the silicate and aluminosilicate networks. The Raman spectra were characterized by increased intensities of Si-O-Pb peaks and decreased intensities of Q^3 peaks with increased PbO contents and showed no evidence of BO_3 or BO_4 ring species. Both the NMR and the Raman data point toward systems where lead is increasingly incorporated into the B_2O_3-SiO_2 and the B_2O_3-SiO_2-Al_2O_3 networks at high PbO concentrations, with the addition of Al_2O_3 enhancing the trend.

TOC graphic

April M. Sawvel, Sarah C. Chinn, William L. Bourcier, and Robert S. Maxwell*

Chem. Mater. **200x**, *xx*, xx

Local Structure of Amorphous $(PbO)_x$ $[(B_2O_3)_{1-z}(Al_2O_3)_z]_y(SiO_2)_y$ Dielectric Materials by Multinuclear Solid State NMR

Glasses in the series $(PbO)_x$ $[(B_2O_3)_{1-z}$ $(Al_2O_3)_z]_y(SiO_2)_y$ have important applications as mixed oxide dielectrics due to their broad range of tailorable physical properties. These properties are in no small part due to the influences of chemical speciation. In this paper we use multinuclear NMR and Raman spectroscopy to produce insight into the structural changes that occur with the addition of aluminum to lead borosilicate glasses - the first such study in this quaternary glass system.

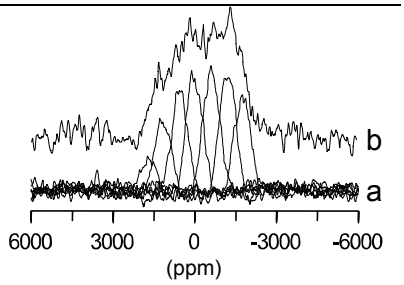

Introduction

The physical properties of lead alumino-borosilicate, $(PbO)_x$ $[(B_2O_3)_{1-z}$ $(Al_2O_3)_z]$ $_y$ (SiO_2) $_y$, where y = (1-x)/2, glasses lend themselves to a wide variety of commercial applications, such as Mixed Oxide Dielectrics (MODs), thick film technology ink constituents, and hosts for

fluorescence centers in optical devices. In such applications, optimal engineering performance is dominated by the glass structure. In Ho^{3+} doped systems, for example, the optical adsorption and fluorescence properties have been found to be strongly correlated to small changes in the glass speciation.[1] Lead borosilicate films deposited on alumina surfaces have been observed to be more prone to devitrification, presumably due to the incorporation of network modifying Al^{3+} species.[2] In addition, the number of non-bridging oxygen atoms can be correlated to the activation energy for d.c. conduction.[3] These examples illustrate that optimized engineering of component physical and electric properties can be facilitated by having an understanding of the structure-property relationships in these materials.

Structural investigations have been previously reported for glasses in the series $PbO\text{-}SiO_2$ and $PbO\text{-}B_2O_3\text{-}SiO_2$.[1-16] These studies, among others, have demonstrated that solid-state nuclear magnetic resonance can be a very effective spectroscopic method for quantitative structural characterization of these amorphous solids in the general family of silica based, multi-component glasses.[11] NMR studies conducted by Fayon et al. on lead silicate glasses[4] indicated that covalently bonded lead is always present within the glass system, even though its role as network former and modifier changes with sample composition. The authors reported that at low lead concentrations, lead was concentrated in small, covalent clusters with SiO_4 tetrahedra being the main glass former. With increased lead content, lead clusters begin to merge and the SiO_4 network breaks down, leaving the lead structure as the main glass former. Fayon et al. also conducted XAFS experiments, which further supported these conclusions.[5]

Previous studies of the $PbO\text{-}B_2O_3\text{-}SiO_2$ system[1-2,4-10] have shown that lead has a dual role as both network former and network modifier. At low concentrations (below 50 mol%) the majority of lead formed an ionic, network modifier species. At higher concentrations, lead behaved as a network former and more covalent bonding of lead was observed. At concentrations of 50 mol%, lead was equally distributed between modifier and former species. This trend was observed to be independent from changes in any of the other constituents present in the glass system. In the studies conducted by Kim et al.[6], it was suggested, but not

confirmed, that Pb^{2+} ions present at low lead concentrations had a bonding preference to the boron-oxygen networks over the silicon-oxygen networks, allowing conversion of a substantial amount of the BO_3 units to BO_4 units.

It is well known that changes in speciation within the glass network with even small changes in composition or processing can have large effects on the physical, electrical, and other material properties of amorphous materials. In the case of lead borosilicate and lead alumino-borosilicate glasses, changes in composition (especially PbO concentration) can lead to drastic changes in sintering densities, resistivity, temperature instabilities, microwave properties, microhardness, viscosity, glass transition temperature, and photoconductive properties.[17-26] NMR and IR studies by Sudarsan et al. show that changes in the boron and lead contents have a dramatic effect on the bonding arrangements and material properties of borosilicate glasses.[27] Despite the ability of NMR methods to assess speciation changes in multicomponent glasses, no NMR studies have been reported on lead alumino-borosilicate glasses. In this paper, we use NMR data on PbO-B_2O_3-SiO_2, PbO-B_2O_3-Al_2O_3-SiO_2, and PbO-Al_2O_3-SiO_2 glass systems to produce insight into the structural changes that occur with the addition of aluminum to lead borosilicate glasses.

Experimental Section

Materials. Nine samples in the composition range $(PbO)_x\ [(B_2O_3)_{1-z}\ (Al_2O_3)_z]_{\ y}\ (SiO_2)_{\ y}$, where x = 0.35, 0.5, and 0.65, y=(1-x)/2, and z = 0.0, 0.5 and 1.0 were prepared. However, only seven of the nine samples formed a glass. The chemical compositions of each sample are listed in Table 1. Reagent grade lead (II) oxide, boric acid (H_3BO_3), silica (SiO_2), and aluminum hydroxide ($Al(OH)_3$) were weighed out and mixed in 1.0 L polystyrene containers. The powder mixture was then transferred to a platinum crucible and melted using a high temperature electric furnace in air. Melting temperatures ranged from 1000°C to 1550°C. Each sample was placed in the furnace at 500°C and allowed to sit for one hour to drive off any water that may have been adsorbed to the surface of the reagents. The temperature was then raised to the final

melting temperature and the samples were stirred periodically to ensure thorough mixing of the components during the melting process. Each sample was left at the melting temperature for a minimal amount of time to prevent lead volatilization. Once melted, the samples were quenched by pouring directly onto a clean metal block. Finally, the samples were crushed in air using a mortar and pestle.

The 50 mol% PbO lead borosilicate glass was selected as a representative sample to test the stability of the materials as well as the accuracy of the compositions. Thermogravimetric analysis (TGA) and inductively coupled plasma optical emission spectroscopy (ICP-OES) were both performed on the sample. TGA showed a weight loss of 0.33% over a temperature range of 0-1000 $^{\circ}$C, indicating that the only water present was adsorbed to the surface of the glass. Elemental compositions of the samples were verified with ICP-OES, performed by Galbraith Laboratories, Inc, (Knoxville, TN). Powder X-ray diffraction verified the absence of crystallinity within the materials reported in this study.

NMR. ^{207}Pb NMR of lead oxides, in general, is characterized by large chemical shift anisotropies (CSA) and large distributions of chemical shift due to the dramatic effect even small changes in bond angles and distances can have on the chemical shift.[4] As a result, the ^{207}Pb NMR is commonly so broad that the entire lineshape cannot be observed quantitatively by recording the NMR spectrum with only one frequency. This is often overcome by using a spin-echo mapping approach.[4] The static ^{207}Pb NMR experiments were carried in frequency steps of 40 kHz with inter-pulse delays of either 500 or 250 μs. The pulse length was approximately 6 μs and a 90^{o} calibration experiment was performed before each run, while referencing to $PbNO_3$. A Chemagnetics CMX 300 and a 7.5 mm CPMAS probe tuned to 62.4 MHz ± N*40kHz were used and the experimental delay was set to 120 s. The final spectra were taken as a sum of spectra obtained for each offset, after they were shifted in frequency corresponding to the frequency offset used to acquire the data. An illustration of this is shown in Figure 1.

^{11}B NMR experiments were carried out on a Bruker DRX 500 using a DOTY Scientific 4 mm HXY MAS probe that had no ^{11}B background. Bloch decay experiments were run at spinning speeds of 12 kHz, pulse lengths of 1.1 μs, and a repetition delay of 2 s. The spectra frequency was set to 160.45 MHz and the pulse length was chosen to be approximately 1/10 of the non-selective π/2 pulse length for aqueous H_3BO_3 (10.75 μs). Peak assignments (see the results section below) were made according to previous literature studies.[6,9,28-31] Spectral deconvolutions using DmFit version 2002 software were used to establish the relative quantities of BO_3 and BO_4 units.[32] In all cases the BO_4 species could be fit to a single Gaussian resonance while the BO_3 species were fit using the following values consistent with those for non-ring, BO_3 species with all three oxygen atoms being bridging (C_q = 2.5 ± 0.1 MHz and η = 0.14 ±0.1).[6,9,28-31] Errors in quantitation were derived from fitting three replicate peaks on one sample. Additional ^{11}B NMR experiments were carried out on a Bruker Avance 400 using the same DOTY Scientific 4 mm HXY MAS probe. Bloch decay experiments were run at spinning speeds of 12 kHz, pulse lengths of 0.7 μs, and a repetition delay of 1 s. The spectral frequency was set to 128.37 MHz and the pulse length was chosen to be approximately 1/10 of the non-selective π/2 pulse length for aqueous H_3BO_3 (7.0 μs). Chemical shifts were referenced to aqueous H_3BO_3 at 19.6 ppm.

^{27}Al magic angle spinning (MAS) experiments were completed on a Bruker DRX 500 using a Bruker 4 mm CPMAS probe. The spectral frequency was set at 130.4 MHz. A pulse length (0.65 μs) of approximately 1/10 the non-selective 90° (6.5 μs) was used to assure quantitative results. Shifts were referenced to 1.0M $Al(NO_3)_3$ at 0 ppm. Additional ^{27}Al MAS experiments on the 35 mol% PbO and the 50 mol% PbO aluminum containing samples were run on a Bruker Avance 400 using a Bruker 4 mm CPMAS probe tuned to 104.2 MHz. A pulse length (0.4 μs) of approximately 1/10 the non-selective 90° (4.0 μs) was used to assure quantitative results. Shifts were referenced to 1.0M $Al(NO_3)_3$ at 0 ppm. ^{27}Al Triple Quantum MAS (3QMAS) experiments were run on a Bruker Avance 400 using a Bruker 4 mm CPMAS probe tuned to 104.2 MHz. A standard two pulse z-filtered pulse sequence was used.[33] The non-selective 148

kHz π/2 pulse length was 1.75 μs at the power levels used. The conversion pulse was optimized at 2.5 μs, the reconversion pulse optimized to 0.8 μs. The z-filter pulse was 20 μs after the reconversion pulse and was set to 50 μs with 30 dB of additional attenuation on the RF power level. Data were acquired and processed using the States method and the data was shear transformed in the indirect dimension according to Massiot, et al.[34] The resonance frequency was set to the frequency of $Al(H_20)_6^{3+}$ (0 ppm). Quadrupole coupling parameters, δ_{iso} and P_q, were derived from the both the unsheared spectra according to Fernadez, et al. [35] and from the field dependence of the chemical shifts according to Samoson.[36]

^{29}Si MAS experiments were carried out using a Chemagnetics CMX 300 and a 7.5 mm CPMAS probe tuned to 59.4 MHz. The 90^o pulse was set to 7.5 μs, followed by data acquisition without high powered proton decoupling. Average spinning speeds were 3-4 kHz and the experimental delay was 300 s. Chemical shifts were referenced to the ^{29}Si shift of TMS at 0 ppm.

Raman Spectroscopy. Raman spectra were recorded on a Jobin Yvon Horiba model T64000 using an argon laser as the excitation source. The 514.532 nm wavelength laser line was used and the power output was 170 mA. The detector was oriented in a 180^o geometry and each spectrum was an average of 30 scans from 10 to 1500 cm^{-1}.

Results

^{207}Pb NMR. The ^{207}Pb NMR spectra for all samples exhibited a single broad peak with a center of mass that was dependent on composition (Fig. 2a-g). The width of the resonances in all cases were on the order of 4000 ppm due to the large distributions of chemical shifts and to the typically large CSA expected for lead oxides.[4,10] Such broad static NMR spectra in amorphous lead oxides have been reported previously and resolution of an isotropic chemical shift is difficult, if not impossible.[4,10] Trends in the average bonding arrangement, as a result, are regularly obtained from correlations of the average chemical shift to the shifts derived from detailed studies of crystalline lead model compounds.[4,10] In general, these relationships predict

that ionic lead sites have large negative (shielded) chemical shifts, as in $PbNO_3$ (shift at -3500 ppm), while lead sites characterized by covalently bonded lead have large positive (deshielded) lead chemical shifts (Pb_2O_3 at 2000 ppm). For example, the 35 mol% PbO lead borosilicate glass sample (Figure 2a) was centered slightly upfield of zero chemical shift, indicating a small surplus of ionic bonding. The broad resonance observed for the 50 mol% PbO (Figure 2b) was observed to be deshielded with respect to the 35 mol% sample and the resonance for the 65 mol% sample (Figure 2c) was deshielded relative to the 50 mol% sample. This trend is designated by the dotted line connecting the center of mass for the spectra in Figure 2a-c. These results indicate that covalent lead bonding was the most abundant species at high lead contents and that as the lead content decreased, lead speciation became more ionic in character with the formation of an increased amount of Pb^{2+} network modifier species. Results for the lead borosilicate glasses are largely consistent with the findings of Fayon et al.[4]

The ^{207}Pb spectra for the lead alumino-borosilicate glasses, in which half of the boron present in the borosilicate glasses was replaced by aluminum, are shown in Figures 2d-f. The same shift from ionic bonding to covalent bonding was observed with increased PbO content, though it was more pronounced with the addition of Al_2O_3. This is demonstrated by the more dramatic slope of the dotted line connecting the centers of mass of the spectra in Figures 2d-f. The difference between chemical shift center of gravity for the 35 mol% and 65 mol% PbO borosilicate samples was observed to be approximately 900 ppm, while the difference in center of gravity for the alumino-borosilicate samples of the same composition was observed to be approximately 1700 ppm. These results indicate that the addition of aluminum to the glass matrix with PbO contents above 50 mol% leads to a decrease in the amount of Pb^{2+} modifier species and a stabilization of the glass network.

The sample with 65 mol% PbO was the only sample of the lead aluminosilicate system that formed a glass at the melt temperatures used in this study. It is possible, given the high temperatures required to melt Al_2O_3, these compositions may have formed glasses if melted at higher temperatures. The results from the ^{207}Pb spectrum for the aluminosilicate glass are shown

in Figure 2g and were very similar to those of the 65 mol% sample in the alumino-borosilicate system, reflecting the increased amount of covalent PbO bonding necessary to stabilize the glass network in the absence of B_2O_3.

^{11}B NMR. ^{11}B MAS NMR spectra of the borosilicate and alumino-borosilicate samples are shown in Figures 3a-g and contain two resonances. The spectra are in general agreement with those seen in previous oxidic glass systems with boron oxide constituents.[6,9,28-31] In accordance with these studies, the broader, asymmetric peak centered near 11 ppm has been assigned to trigonal, non-ring, BO_3 units with all of the oxygen atoms bridging, and the sharper peak near 0 ppm is assigned to tetrahedral BO_4 units.[6,28-29] The ^{11}B spectra for the lead borosilicate glasses are shown in Figure 3a-c and were consistent with Kim et al.[6] As the lead content increased, there was an increase in the amount of BO_3 units as well as a small increase in both the BO_3 and BO_4 chemical shifts. This trend implies that as lead content increased, lead became increasingly incorporated into the boron network via B-O-Pb bonding. The differences in $\delta_{11.7T}$ and $\delta_{9.4T}$ were equivalent, within error, indicating that the $\Delta\delta_B$ was not due to lead dependent changes in the quadrupolar coupling parameters. Though deshielding of ^{29}Si chemical shifts with the incorporation of lead into the second coordination sphere has been observed previously, no similar observations have been made for boron. The ^{11}B spectra for the lead alumino-borosilicate glasses are shown in Figure 3d-f and had a much higher percentage of BO_3 units present than the lead borosilicate glasses. For equal PbO concentrations, the percentage of BO_3 units increased with lead content, and at 65 mol% PbO, only a very small amount of BO_4 units were present. Again, there was a small increase in both the BO_3 and BO_4 chemical shifts with increased PbO contents, signifying a greater degree of B-O-Pb species with increasing lead concentration.

In order to assess quantitatively the changes seen in the ^{11}B NMR data, the contribution of each species was determined by spectral deconvolutions using previously published quadrupole coupling parameters (see experimental section).[6,9] For all samples, fits completely reproduced the experimental spectra using only the trigonal, non-ring BO_3 and tetrahedral BO_4 sites. A

value, N_4, was taken as the relative amount of four coordinate boron species present and then plotted against PbO concentration.[6] Figure 4 demonstrates quite clearly that the number of BO_4 units decreased in conjunction with increased amounts of covalently bonded PbO as well as with the addition of aluminum to the glass system.

^{27}Al NMR. The ^{27}Al MAS NMR spectra for the PbO-SiO_2-Al_2O_3-B_2O_3 samples are shown in Figure 5a-c. 2D 3QMAS spectra for the 35% and 65% PbO samples are shown in Figure 6a-c. The spectra, in general, had a single resonance consistent with four-coordinate aluminum that fell in the chemical shift range for framework aluminosilicates, where the silicon and aluminum tetrahedra are joined at the vertices throughout the network.[11] In all three samples, the tetrahedral resonance could be characterized by an upfield non-Gaussian tail due to distributions in the quadrupolar coupling. As observed in the ^{11}B NMR spectra, more deshielded signals were observed with increasing PbO contents. Again, no significant differences in $\Delta\delta_{11.7T\text{-}9.4T}$ were observed as a function of PbO content within experimental error (±0.5 ppm). This supports that idea that the $\Delta\delta_{Al}$, with respect to aluminum content, was not due to lead dependent changes in the second order contribution to the observed chemical shift and was instead due to changes in the isotropic chemical shift. (From analysis of the 3QMAS experiments and the field dependent studies, P_Q for all glasses was determined to be 2.1±0.5 MHz. The isotropic chemical shifts, δ_{iso}, were determined to be as follows: 57.2±0.5 ppm [35%], 59.2±0.5 ppm [50%], and 60.1±0.5 ppm [65%].) These results are consistent with an intermixing of the lead and aluminum oxide species with increased PbO contents.

It is interesting to note that the 35 mol% PbO sample (Figure 5c) exhibited two differences from the 50% and 65% PbO samples. The first difference was the significantly broader shoulder of the tetrahedral resonance and the second difference was the presence of six coordinate aluminum (feature near 0 ppm) and possibly five coordinate aluminum (shoulder at ~ 30 ppm). ^{27}Al 3QMAS was employed to verify the presence of and to resolve the three resonances. The ^{27}Al 3QMAS spectrum of the 35% PbO sample (Figure 6a) clearly shows two

isotropic resonances assignable to four and six coordinate aluminum oxide species. Significant spectral intensity can also be observed in the region for five coordinate aluminum species. The broadening of the four coordinate resonance in the isotropic dimension of the 3QMAS spectrum validates that the foremost broadening factor for the four coordinate resonance is due a combination of a distribution of quadrupolar couplings and chemical shifts.[35] The five and six coordinate aluminum resonances are narrow in the isotropic dimension, though the signal to noise is insufficient to make clear conclusions.

^{29}Si NMR. The ^{29}Si MAS NMR spectra of the glasses studied are shown in Figure 7a-g. In all cases, the spectra were characterized by broad resonances with chemical shifts in the range of –50 to –100 ppm with the mean isotropic chemical shifts becoming less shielded as lead contents increased. Such broad featureless resonances in multicomponent oxide glasses are common and limit the amount of structural insight that can be extracted. Reports on detailed deconvolution of ^{29}Si MAS spectra of both PbO-SiO_2 and B_2O_3 doped PbO-SiO_2 glasses using a number of complex assumptions have been made.[4,25,27] However, the added complexity of the glasses studied here (due to the increased concentration of B_2O_3 and the presence of Al_2O_3 in the lead alumino-borosilicate samples) limit the unambiguous insight that might be garnered from such an approach. The spectra for the glasses in the lead borosilicate series (Figure 7a-c) show a systematic increase in chemical shift of the center of mass of the broad resonances, δ_{CM}, with increasing lead content (δ_{CM} [35%PbO] = -92 ppm, δ_{CM} [50%PbO] = -82 ppm, δ_{CM} [65%PbO] = -78 ppm). In addition, the ^{29}Si resonance for the 35% PbO sample is significantly broader than the resonance for the 65% PbO sample ($\Delta\nu_{35}$ =35 ppm; $\Delta\nu_{50}$ = 30 ppm; $\Delta\nu_{65}$ = 20 ppm). According to empirical correlations between structure and chemical shift trends,[4,11] the borosilicate spectra (Figure 7a-c) are consistent with a decrease in the contribution of Si-O-Si bonding species and an increased formation of Si-O-X species, where X is B, Al, Pb, or non-bonding oxygen, in the glass network. It has been reported that lead in the second coordination sphere as a network former (forming an increased concentration of Si-O-Pb species) may be expected to increase the ^{29}Si chemical shift by approximately 20 ppm.[4] The observed increase

of network forming lead species in the ^{207}Pb NMR with increased PbO contents and the dramatic increase in ^{29}Si chemical shifts with increased PbO contents indicate an intermixing of lead in the silicon bonding network.

The ^{29}Si spectra for the lead alumino-borosilicate glasses are shown in Figure 7d-f. The mean chemical shift for these glasses was shifted approximately 10 ppm downfield when compared to the lead borosilicate glasses of comparable Pb/Si ratios. This is consistent with the expected influence of aluminum on the local silicon environment if incorporated in the second coordination sphere.[11] The spectra were also characterized by a systematic change in the ^{29}Si chemical shift with increased PbO contents, representing incorporation of Pb into the aluminosilicate matrix at high PbO concentrations (δ_{CM} [35%PbO] = -75 ppm, δ_{CM} [50%PbO] = -65 ppm, δ_{CM} [65%PbO] = -59 ppm). In addition, the linewidths for these spectra are similar and do not narrow as was observed in the lead borosilicate system (Figure 7d-f). This is most likely due to the broader distribution of species in the alumino-borosilicate network.

Raman Data. Raman spectra for the lead borosilicate, the lead alumino-borosilicate, and the lead aluminosilicate glasses are shown in Figure 8a-g. Peak assignments for the Raman spectra were made based on trends observed in related binary and tertiary glass systems.[21,37-38] Although Raman spectra were acquired from 10-1500 cm^{-1}, the high intensity, low-frequency boson peak[38] and the PbO vibrational peak present in the glasses with higher lead concentration[21] are omitted from this figure. The only observable change in this region was the previously reported PbO peak splitting which occurs with increased PbO contents as the glass changes from a random to a more ordered symmetry.[38]

The peaks near 600, 690, and 850-950 cm^{-1} were assigned to vibrations within the Si-O-Pb network. The peak intensities in the lead borosilicate spectra (Figure 8a-c) increased with increasing PbO contents, indicating higher concentrations of Si-O-Pb network species which supports the data from both the ^{207}Pb and ^{29}Si NMR results. The small peak appearing near 1100 cm^{-1} in the lead borosilicate spectra (Figure 8a-c) was attributed to symmetric Si-O vibrations of non-bridging oxygens in Q^3 units.[37] The decrease in peak intensity with increased

PbO contents is consistent with the ^{29}Si MAS NMR data reported here (Figure 7a-c) where signal deshielding with increased PbO contents represents a decrease in Q^3 species. These results are also consistent with ^{29}Si MAS NMR results reported by Sudarsan, et al., Fayon, et al., and Shrikande, et al.[4,25,27] Finally, the vitreous B_2O_3 peak centered between 1200 and 1300 cm^{-1} (Figure 8a-f) has been attributed to network forming boron species and follow trends observed in lead borate glasses by Witke et al.[38] Witke associated this broad peak with a delocalized B-O scattering continuum and observed a decrease in the peak frequency from above 1350 cm^{-1} to below 1300 cm^{-1} as lead contents increased above 30 mol% PbO. The Raman data presented here for the lead borosilicate samples show the peak frequency of the 35 mol% PbO sample (Figure 8a) at ~1350 cm^{-1} shift to ~1300 cm^{-1} at 50 mol% PbO (Figure 8b) and, finally, down to ~1250 cm^{-1} for the 65 mol% PbO sample (Figure 8c). The Raman data show no sign of six-membered boroxol rings (expected at 805 cm^{-1}) or six-membered borate rings (770 cm^{-1}), which is in agreement with the ^{11}B NMR data.

The formation of a Pb-O-Si network is also manifest in the Raman data of the alumino-borosilicate glasses (Figure 8d-f). However, the Raman signals are significantly lower in intensity than in the corresponding borosilicate glasses (Figure 8a-c) due to the decreased amount of boron present in the alumino-borosilicate samples. The shift in the vitreous B_2O_3 peak from approximately 1260 cm^{-1} to approximately 1200 cm^{-1} in the alumino-borosilicate samples (Figure 8d-f) with increasing PbO concentration is attributed to the increasing formation of B-O-Pb bonds, which is consistent with the ^{11}B and the ^{207}Pb NMR.

Discussion and Conclusion

Lead Borosilicates. In general, the trends observed here for the borosilicate glasses followed those observed by Kim et al. and Fayon et al.[4,6] At low PbO content, ionic lead oxide was the most abundant lead species. As the lead contents were increased from 35 mol% to 65 mol% PbO, the ^{207}Pb spectra showed a decrease in the amount of network modifying lead present (Pb^{2+}) and an increase in the covalent, network forming lead oxide species. Presumably,

the lead became more thoroughly integrated in the glass network as this change occurred. Though the B_2O_3 and SiO_2 contents decreased with increasing lead contents, the B/Si ratio remained constant. The ^{11}B MAS NMR showed both an increased presence of BO_3 units and a systematic downfield shift with increasing lead contents, indicating that the lead network stabilized BO_3 units at the expense of BO_4 species and that the lead and boron species were within close proximity. These observations are consistent with other systems where increased incorporation of the metal species into the network (here evidenced by increasingly deshielded chemical shifts for ^{11}B, ^{207}Pb, and ^{29}Si) leads to the stabilization of BO_3 species.[9,39-40] The ^{29}Si spectra showed a downfield shift and a decreasing linewidth with increasing lead contents, indicative of a greater degree of lead incorporation in the silicon network and homogenization of the silicon speciation. The Raman data showed an increase in peak intensities associated with Si-O-Pb vibrations and a decrease in peak intensities associated with Q^3 silicon species with increasing lead contents. The increase in covalently bonded lead, the increase in BO_3 sites, the movement of the mean isotropic chemical shift in the ^{29}Si spectra, the sharpening of the ^{29}Si linewidths, and the decrease in intensity of the Q^3 peak in the Raman spectrum with increasing PbO contents all suggest that lead becomes more homogeneously incorporated into the network through Si-O-Pb and B-O-Pb bonds at very high lead contents.

Lead Alumino-borosilicates. All of the NMR results indicated that the addition of aluminum to the borosilicate network caused noticeable changes in the overall glass network. In general, the trends observed in the lead borosilicate system were also found here. Specifically, the ^{207}Pb, ^{11}B, and ^{29}Si chemical shifts were more deshielded with increased PbO concentration. The ^{11}B MAS NMR again showed a decrease in the BO_4 population with increased PbO content. The ^{27}Al MAS NMR also showed a more deshielded chemical shift with increasing PbO contents. In all cases, however, the magnitude of these changes as a function of PbO contents was greater in the lead alumino-borosilicate system than the lead borosilicate system. The BO_4 concentrations were much lower for the lead alumino-borosilicate system due to the higher affinity of the Al_2O_3 network for non-bridging oxygen species. The promotion of BO_3

species with the addition of Al_2O_3 has also been observed previously in the CaO-Al_2O_3-B_2O_3 and TeO_2-B_2O_3-Al_2O_3 system.[41-42] Finally, the ^{29}Si linewidths in the lead alumino-borosilicate system were larger than in the lead borosilicate system due to the broader distribution of species. The NMR and Raman data shown here suggest that increased lead contents drive lead into the B_2O_3-SiO_2 and B_2O_3-SiO_2-Al_2O_3 networks and that this trend is increased with the addition of Al_2O_3 to the network.

Acknowledgement. This work was performed under the auspices of the U.S. Department of Energy by the UC, Lawrence Livermore National Laboratory under contract # W-7405-ENG-48.

References

(1) Reddy, M.R.; Raju, S.B.; Veeraiah, N. *J. Phys. Chem. Solids* **2000**, *61*, 1567.

(2) Prudenziati, M.; Morten, B.; Forti, B.; Gualtieri, A.F.; Dilliway, G.M. *J. Inorg. Mat.* **2001**, *3*, 667.

(3) Gough, E.; Isard, J.O.; Topping, J.A. *Phys. Chem. Glasses* **1969**, *10*, 89.

(4) Fayon, F.; Bessada, C.; Massiot, D.; Farnan, I.; Coutures, J.P. *J. Non-Cryst. Solids* **1998**, *232-234*, 403.

(5) Fayon, F.; Landron, C.; Sakurai, K.; Bessada, C.; Massiot, D. *J. Non-Cryst. Solids* **1999**, *243*, 39.

(6) Kim, K.S.; Bray, P.J.; Merrin, S. *J. Chem. Phys.* **1976**, *64*, 4459.

(7) Stentz, D.; Blair, S.; Goater, C.; Feller, S.; Affatigato, M. *J. Non-Cryst. Solids* **2001**, *293-295*, 416.

(8) Wang, P.W.; Zhang, L. *J. Non-Cryst. Solids* **1996**, *194*, 129.

(9) Bray, P.J.; Leventhal, M.; Hooper, H.O. *Phys. Chem. Glasses* **1963**, *4*, 47.

(10) Fayon, F.; Farnan, I.; Bessada, C.; Coutures, J.; Massiot, D.; Coutures, J.P. *J. Am. Chem. Soc.* **1997**, *119*, 6837.

(11) Engelhardt, G.; Michel, D. *High-Resolution Solid-State NMR of Silicates and Zeolites*; John Wiley & Sons: Chinchester, 1987.

(12) Wright, A.C.; Vedishcheva, N.M.; Shakhmatkin, B.A. *J. Non-Cryst. Solids* **1995**, *192-193*, 92.

(13) Zahra, A.-M.; Zahra, C.Y. *J. Non-Cryst. Solids* **1993**, *155*, 45.

(14) Bessada, C.; Massiot, D.; Coutures, J.; Douy, A.; Coutures, J.-P.; Taulelle, F. *J. Non-Cryst. Solids* **1994**, *168*, 76.

(15) Yoko, T.; Tadanaga, K.; Miyaji, F.; Sakka, S. *J. Non-Cryst. Solids* **1992**, *150*, 192.

(16) Mao, D.; Bray, P.J. *J. Non-Cryst. Solids* **1992**, *144*, 217.

(17) Hwang, G.-H.; Kim, W.-Y.; Jeon, H.-J.; Kim, Y.-S. *J. Am. Ceram. Soc.* **2002**, *85*, 2961.

(18) Adachi, K.; Kuno, H. *J. Am. Ceram. Soc.* **2000**, *83*, 2441.

(19) Vlasov, S.I.; Parchinskiĭ; P.B.; Nasirov, A.A.; Olmatov, B.A. *Tech. Physics* **1999**, *44*, 998.

(20) Wu, J.-M.; Huang, H.-L. *J. Non-Cryst. Solids* **1999**, *260*, 116.

(21) Petrovskaya, T.S. *Glass and Ceramics* **1997**, *54*, 347.

(22) Granier, W.; Jabobker, K.; Pradel, A.; Pham Thi, M. *J. Non-Cryst. Solids* **1992**, *147&148*, 574.

(23) Kobayashi, K.; Mizushima, I. *J. Non-Cryst. Solids* **1994**, *180*, 84.

(24) Sehgal, J.; Ito, S. *J. Non-Cryst. Solids* **1999**, *253*, 126.

(25) Shrikhande, V.K.; Sudarsan, V.; Kothiyal, G.P.; Kulshreshtha, S.K. *J. Non-Cryst. Solids* **2001**, *283*, 18.

(26) Mattox, D.M.; Robinson, J.H. *J. Am. Ceram. Soc.* **1997**, *80*, 1189.

(27) Sudarsan, V.; Shrikhande, V.K.; Kothiyal, G.P.; Kulshreshtha, S.K. *J. Phys.: Condens. Matter* **2002**, *14*, 6553.

(28) Du, L-S.; Stebbins, J.F. *Chem. Mater.* **2003**, *15*, 3913.

(29) Sen, S.; Xu, Z.; Stebbins, J. F. *J. Non-Cryst. Solids* **1998**, *226*, 29.

(30) Zhong, P.; Bray, P. J. *J. Non-Cryst Solids* **1989**, *111*, 67.

(31) Youngman, R. E.; Zwanzinger, J. W. *J. Phys. Chem* **1996**, *100*, 16720.

(32) Massiot, D.; Fayon, F.; Capron, M.; King, I.; Calvé, S.; Alonso, B.; Durand, J.-O.; Bujoli, B.; Gan, Z.; Hoatson, G. *Mag. Reson. Chem.* **2002**, *40*, 70.

(33) Ganapathy, S.; Das, T.K.; Vetrivel, R.; Ray, S.S.; Sen, T.; Sivasanker, S.; Delevoye, L.; Fernandez, C.; Amoureux, J.P. *J. Am. Chem. Soc.* **1998**, *120*, 4752.

(34) Massiot, D.; Touzo, B; Trumeau, D.; Coutures, J. P.; Virlet, J.; Flourian, P.; Grandinetti, P. *J. Solid State Mag. Res*. **1996**, *6*, 73.

(35) Fernandez, C.; Amoureux, J.P.; Chezeau, J.M.; Delmotte, L.; Kessler, H. *Microporous Mat.* **1996**, *6*, 331.

(36) Samoson, A.; *Chem. Phys. Lett.* **1985**, *119*, 29.

(37) Bunker, B.C.; Tallant, D.R.; Kirkpatrick, R.J.; Turner, G.L. *Phys. Chem. Glasses* **1990**, *31*, 30.

(38) Witke, K. Hübert, T.; Reich, R.; Splett, C. *Phys. Chem. Glasses* **1994**, *35*, 28.

(39) Kim, K. S.; Bray, P. J. *Phys. Chem. Glasses* **1972**, *13*, 63.

(40) Baugher, J. F.; Bray, P. J. *Phys. Chem. Glasses* **1969**, *10*, 77.

(41) Bishop, S. G.; Bray, P. J. *Phys. Chem. Glasses* **1966**, *7*, 73.

(42) Harris, I. A.; Bray, P. J. *Phys. Chem. Glasses* **1984**, *25*, 44.

Tables:

Table 1. Chemical compositions of each sample prepared. (*) Indicates that the sample did not form a glass. Sample compositions are based on the starting ratio of oxides.

Sample Compositions				
Sample #	**Mol% PbO**	**Mol% B_2O_3**	**Mol% Al_2O_3**	**Mol% SiO_2**
A	35	32.5	0	32.5
B	50	25	0	25
C	65	17.5	0	17.5
D	35	17	16	32
E	50	13	12	25
F	65	9	8	18
H*	35	0	32.5	32.5
I*	50	0	25	25
G	65	0	17.5	17.5

List of Figures

Figure 1. a. ^{207}Pb single spin echo spectra at variable offsets for $(PbO)_{0.35}(B_2O_3)_{0.325}(SiO_2)_{0.325}$; b. ^{207}Pb cumulative spectrum for $(PbO)_{0.35}(B_2O_3)_{0.325}(SiO_2)_{0.325}$

Figure 2. ^{207}Pb cumulative spectra for all glass samples. The dotted lines serve as a guide for the eye. a. $(PbO)_{0.35}(B_2O_3)_{0.325}(SiO_2)_{0.325}$; b. $(PbO)_{0.50}(B_2O_3)_{0.25}(SiO_2)_{0.25}$; c. $(PbO)_{0.65}(B_2O_3)_{0.175}(SiO_2)_{0.175}$; d. $(PbO)_{0.35}[(B_2O_3)(Al_2O_3)]_{0.33}(SiO_2)_{0.32}$; e. $(PbO)_{0.50}[(B_2O_3)(Al_2O_3)]_{0.25}(SiO_2)_{0.25}$; f. $(PbO)_{0.65}[(B_2O_3)(Al_2O_3)]_{0.17}(SiO_2)_{0.18}$; g. $(PbO)_{0.65}(Al_2O_3)_{0.175}(SiO_2)_{0.175}$

Figure 3. ^{11}B MAS NMR for the lead borosilicate and the lead alumino-borosilicate glasses. a. Spectral deconvolution of $(PbO)_{0.35}(B_2O_3)_{0.325}(SiO_2)_{0.325}$; b. $(PbO)_{0.35}(B_2O_3)_{0.325}(SiO_2)_{0.325}$; c. $(PbO)_{0.50}(B_2O_3)_{0.25}(SiO_2)_{0.25}$; d. $(PbO)_{0.65}(B_2O_3)_{0.175}(SiO_2)_{0.175}$; e. $(PbO)_{0.35}[(B_2O_3)(Al_2O_3)]_{0.33}(SiO_2)_{0.32}$; f. $(PbO)_{0.50}[(B_2O_3)(Al_2O_3)]_{0.25}(SiO_2)_{0.25}$; g. $(PbO)_{0.65}[(B_2O_3)(Al_2O_3)]_{0.17}(SiO_2)_{0.18}$

Figure 4. Four coordinate boron species, N_4, versus lead oxide concentration [PbO]. Unfilled diamonds represent the lead borosilicate glasses and filled diamonds represent lead alumino-borosilicate glasses. Error bars are taken from variation in the fits to replicate data sets and estimated uncertainties in % composition.

Figure 5. ^{27}Al MAS spectra for the lead alumino-borosilicate glasses. (*) Indicate spinning sidebands. a. $(PbO)_{0.35}[(B_2O_3)(Al_2O_3)]_{0.33}(SiO_2)_{0.32}$; b. $(PbO)_{0.50}[(B_2O_3)(Al_2O_3)]_{0.25}(SiO_2)_{0.25}$; c. $(PbO)_{0.65}[(B_2O_3)(Al_2O_3)]_{0.17}(SiO_2)_{0.18}$

Figure 6. 2D sheared ^{27}Al 3QMAS spectrum for the $(PbO)_{0.35}[(B_2O_3)(Al_2O_3)]_{0.33}(SiO_2)_{0.32}$ glass. (*) Indicate spinning sidebands in F1 dimension.

Figure 7. ^{29}Si spectra for all of the glass samples. a. $(PbO)_{0.35}(B_2O_3)_{0.325}(SiO_2)_{0.325}$; b. $(PbO)_{0.50}(B_2O_3)_{0.25}(SiO_2)_{0.25}$; c. $(PbO)_{0.65}(B_2O_3)_{0.175}(SiO_2)_{0.175}$; d.

$(PbO)_{0.35}[(B_2O_3)(Al_2O_3)]_{0.33}(SiO_2)_{0.32}$; e. $(PbO)_{0.50}[(B_2O_3)(Al_2O_3)]_{0.25}(SiO_2)_{0.25}$; f. $(PbO)_{0.65}[(B_2O_3)(Al_2O_3)]_{0.17}(SiO_2)_{0.18}$; g. $(PbO)_{0.65}(Al_2O_3)_{0.175}(SiO_2)_{0.175}$

Figure 8. Raman spectra for all glass samples. a. $(PbO)_{0.35}(B_2O_3)_{0.325}(SiO_2)_{0.325}$; b. $(PbO)_{0.50}(B_2O_3)_{0.25}(SiO_2)_{0.25}$; c. $(PbO)_{0.65}(B_2O_3)_{0.175}(SiO_2)_{0.175}$; d. $(PbO)_{0.35}[(B_2O_3)(Al_2O_3)]_{0.33}(SiO_2)_{0.32}$; e. $(PbO)_{0.50}[(B_2O_3)(Al_2O_3)]_{0.25}(SiO_2)_{0.25}$; f. $(PbO)_{0.65}[(B_2O_3)(Al_2O_3)]_{0.17}(SiO_2)_{0.18}$; g. $(PbO)_{0.65}(Al_2O_3)_{0.175}(SiO_2)_{0.175}$

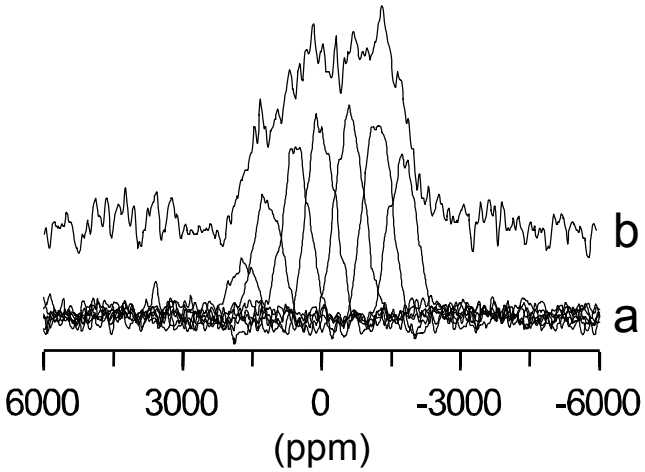

Figure 1.

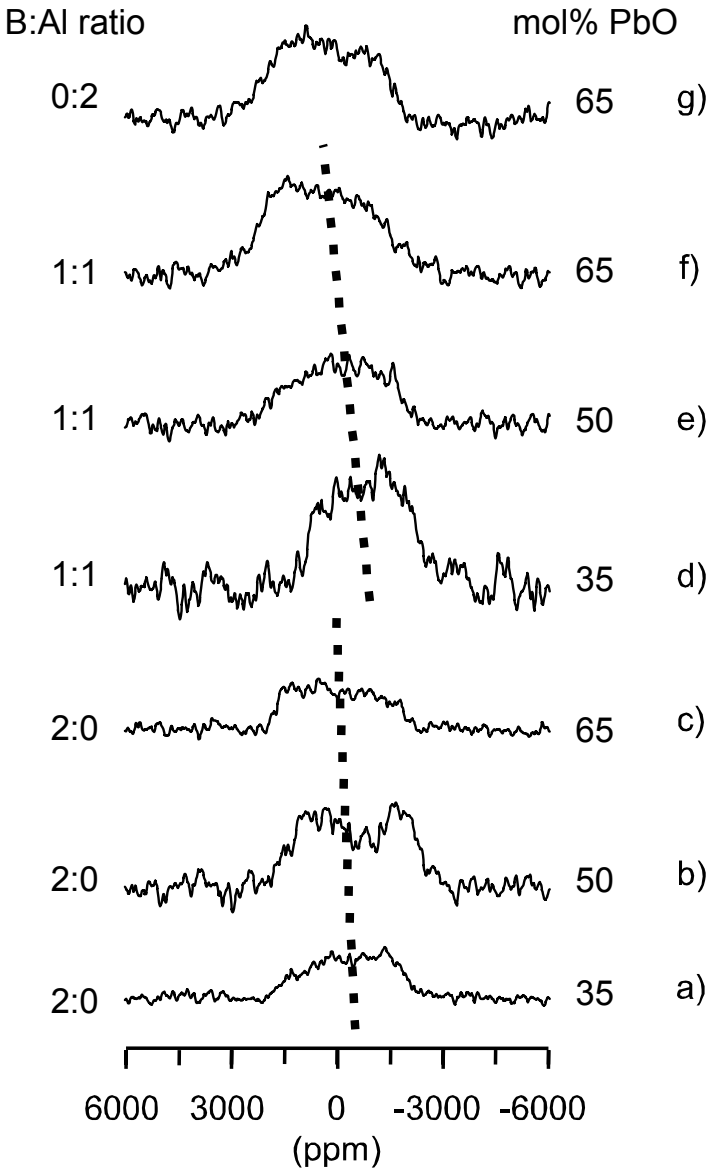
B:Al ratio
mol% PbO
0:2
65
g)
1:1
65
f)
1:1
50
e)
1:1
35
d)
2:0
65
c)
2:0
50
b)
2:0
35
a)
6000
3000
0
-3000
-6000
(ppm)

Figure 2.

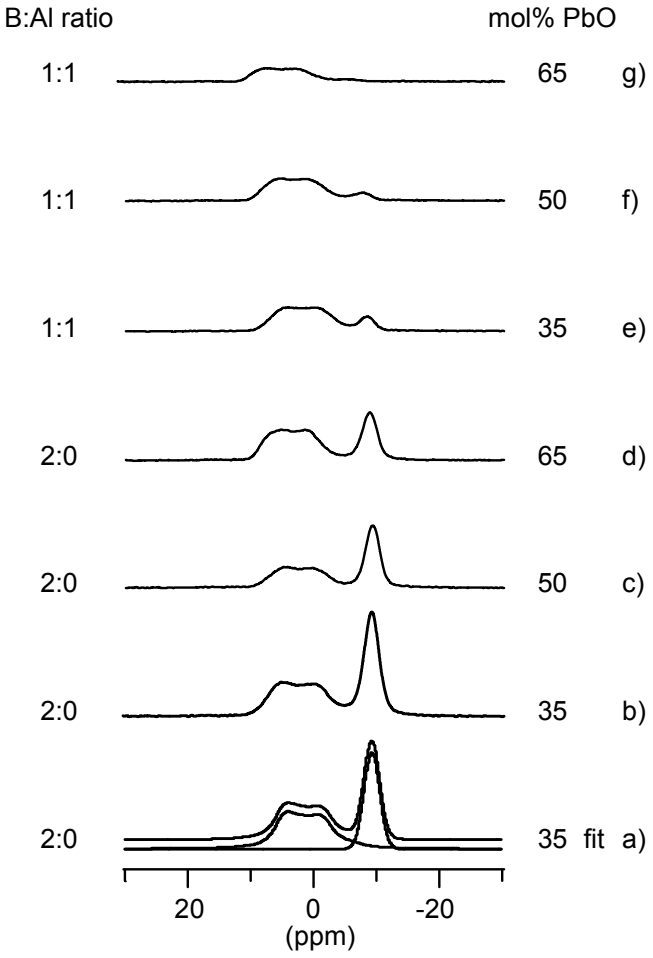
B:Al ratio
mol% PbO
1:1
65
g)
1:1
50
f)
1:1
35
e)
2:0
65
d)
2:0
50
c)
2:0
35
b)
2:0
35 fit
a)
20
0
-20
(ppm)

Figure 3.

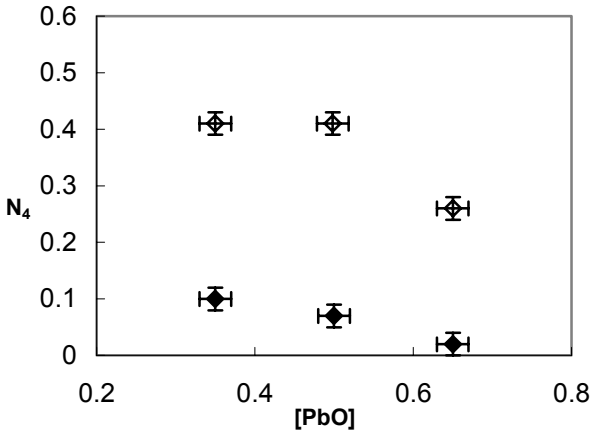

Figure 4.

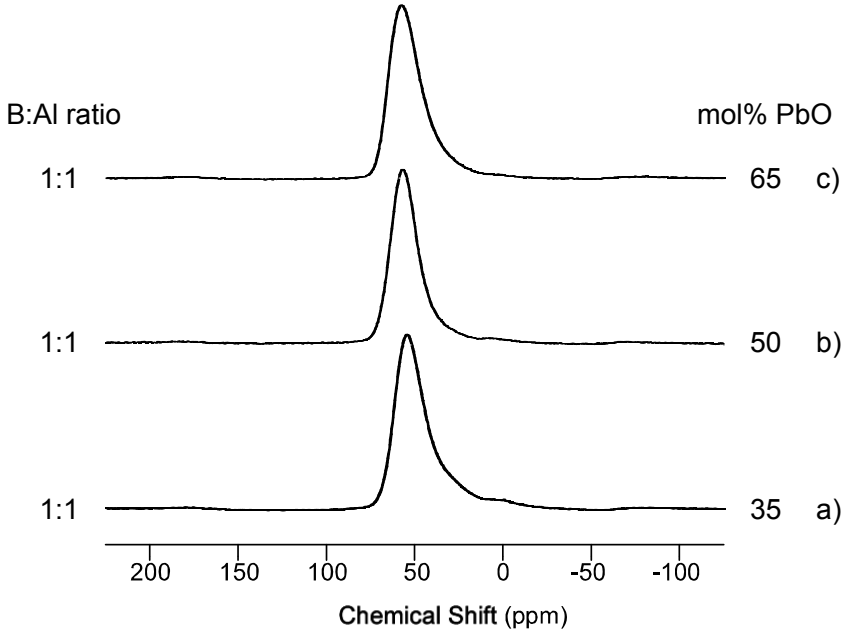
B:Al ratio
mol% PbO
1:1
65
c)
1:1
50
b)
1:1
35
a)
200
150
100
50
0
-50
-100
Chemical Shift (ppm)

Figure 5.

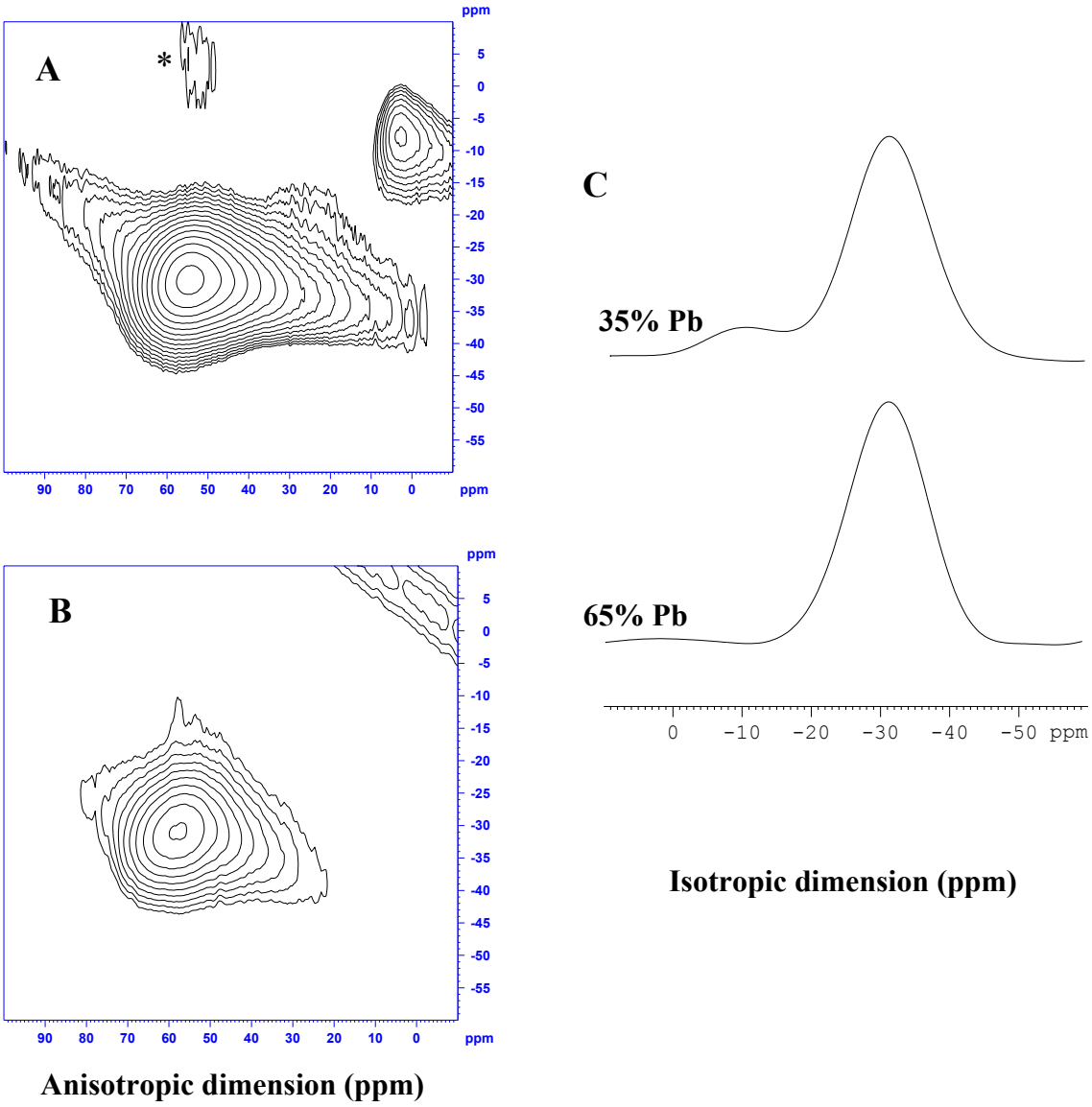
A
*
B
C
35% Pb
65% Pb
ppm
5
0
-5
-10
-15
-20
-25
-30
-35
-40
-45
-50
-55
90 80 70 60 50 40 30 20 10 0 ppm
0 -10 -20 -30 -40 -50 ppm
Anisotropic dimension (ppm)
Isotropic dimension (ppm)

Figure 6.

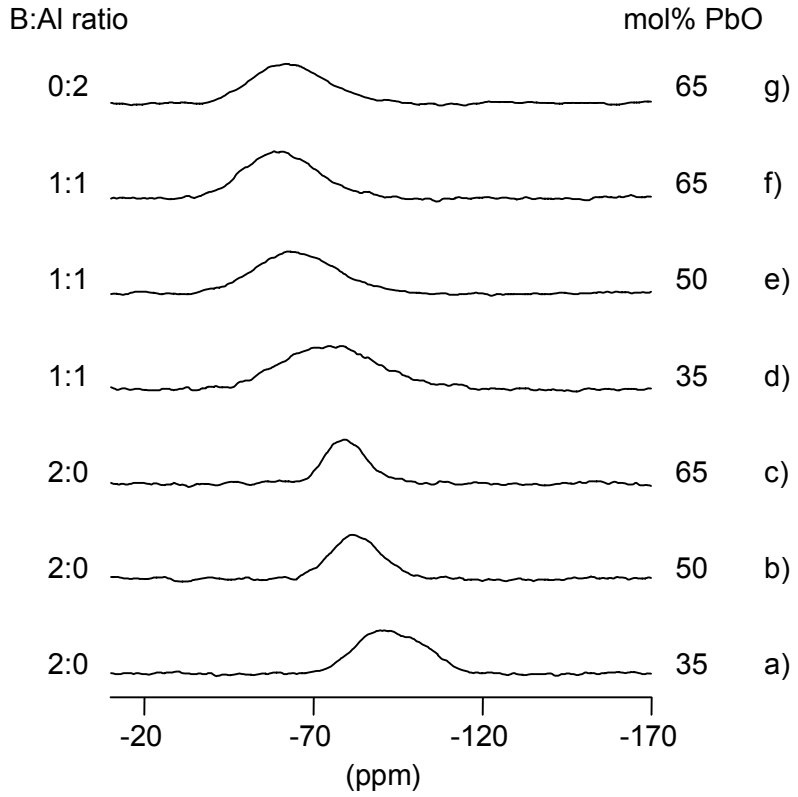
B:Al ratio
mol% PbO
0:2
65
g)
1:1
65
f)
1:1
50
e)
1:1
35
d)
2:0
65
c)
2:0
50
b)
2:0
35
a)
-20
-70
-120
-170
(ppm)

Figure 7.

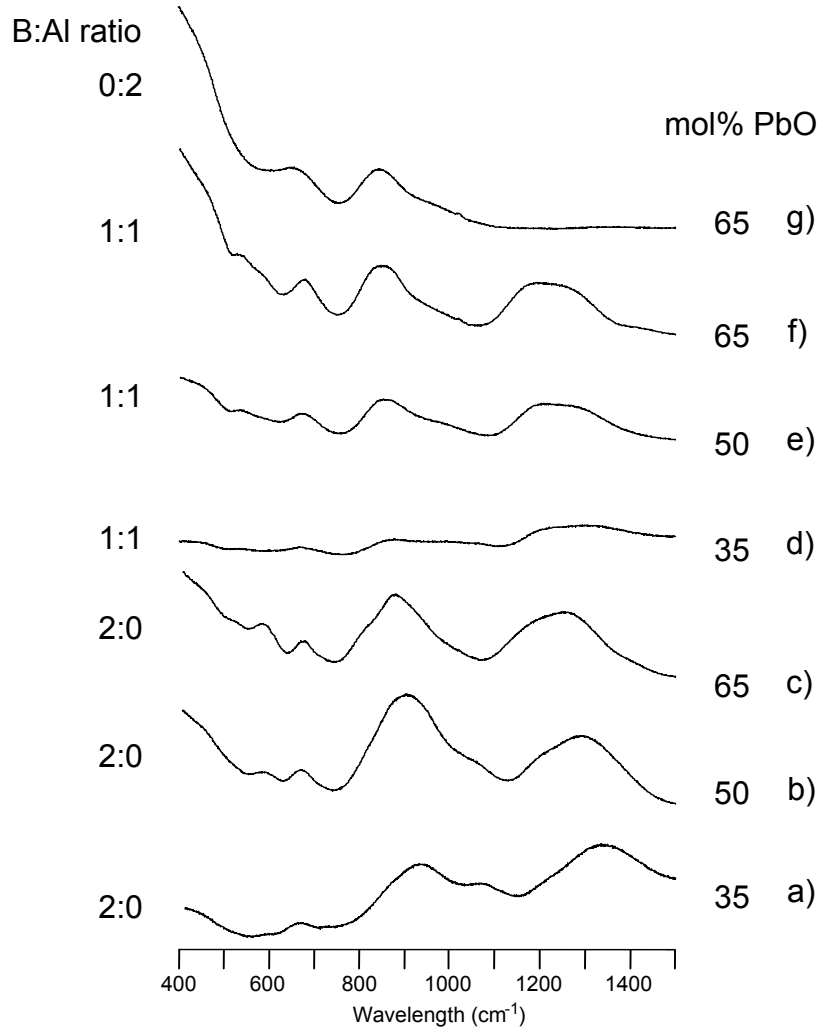
B:Al ratio
0:2
1:1
1:1
1:1
2:0
2:0
2:0
mol% PbO
65 g)
65 f)
50 e)
35 d)
65 c)
50 b)
35 a)
400
600
800
1000
1200
1400
Wavelength (cm-1)

Figure 8.